Mandibular finite helical axis pathway

Review Article

Shilpa Shetty

ABSTRACT

Condylar and incisor trajectories are often used for the study of mandibular movements. Condylar trajectories, however, depend on the location of the reference point and can be interpreted erroneously. In contrast, the helical axis analysis yields an unequivocal description of rigid body kinematics. The finite helical axis (FHA) is a mathematical model which can be used to describe comprehensively the movements of the rigid body.an optoelectronic jaw tracking system, JAWS 3D, was used for this purpose. The finite helical axis were never localized within the condyle and often were located outside the mandible. The analysis of the FHA pathways yields more information on whole mandibular movements than simply the movements of a single condylar point.

KEY WORDS: Biomechanics, finite helical axis, temporomandibular joint

INTRODUCTION

The temporomandibular joint is a compound joint with an upper and lower compartments divided by an articular disc. Mandibular opening and closing movements are performed by a combination of condylar rotation and translation of the condyle-disc complex. In a normal TMJ, the movements between the condyle and the disc are mainly hinge-like, whereas those between the fossa and the condyle-disc complex are translatory.[1-6]

Very few studies have analyzed the relationship between the rotational and translational components during opening and closing.[7-12] The data from these studies indicated that for normal subjects there is a linear relationship between these two components during opening and closing movements, that is, on average, the initial movement started with both rotation and anterior translation and the relationship remained constant throughout opening and closing movements. But this was not always true for subjects with temporomandibular disorders. In these joints which have an initially very steep condylar path, the opening movement started with a pronounced rotation.

These studies on condylar rotation and translation have two main limitations.[13] First, the translatory component was described only in one direction i.e., only anteroposteriorly. This limitation may lead to erroneous conclusion that in the absence of anterior/posterior translation, as in the case of a clicking joints, the condyle only rotates, whereas in fact, the condylar rotation is accompanied by a vertical translation. Second, the rotational component was calculated by measurement of the opening angle between the upper and lower jaws thus ignoring the location of the axis about which the rotation occurs. The location of the axis of rotation is important however, since its spatial position reflects the activation pattern of the masticatory muscles as well as possible abnormalities of the joint

DESCRIPTION OF THE HELICAL AXIS

A more comprehensive analysis of rotation and translation is provided by the description of the helical axis.[13] This analysis also permits a better evaluation and comparision of jaw motion because it describes the movement of the whole mandible and not of single points.

The helical axis model has only recently been introduced into the analysis of mandibular kinematics,[13] in spite of its already widespread use for biomechanical and especially orthopedic studies of other joints. Due to their anatomy, some joints - such as the elbow - rotate around a fixed axis, whereas other joints = such as the

Department of Prosthodontics, V. S. Dental College, Bangalore, India

Address for correspondence: Dr. Shilpa Shetty, 664,17th D main, 6th Block, Koramangala, Bangalore, India. E-mail: drshilpashetty@gmail.com

wrist,[14] the ankle,[15] the knee[16] and the TMJ – rotate around an axis moving in space, best described by helical axis.

The spatial motion of a rigid body, for instance of the mandible, can be described by means of a helical axis (also called twist axis, screw axis, or axis of rotation).[15-20] In this model the infinitesimal motion of the rigid body is expressed as a combination of a translation along an axis in space and a rotation around it, the so-called instantaneous helical axis (IHA). This principle is graphically represented in Figure 1. During the body motion, the IHA describes a continuous pathway that changes position and orientation in space. The finite helical axis (FHA) is the axis calculated between consecutive motion steps, i.e., at discrete time points. By knowing position and orientation in space of the FHA, the rotation around and the translation along it, as well as the coordinates of the body points, the position of the body can be reconstructed at any time.

To visualize the path of the FHA in space during jaw movements, the FHA is expressed in a coordinate system parallel to that of an optoelectronic jaw-tracking system, JAWS-3D, but centered on a preselected condylar point. This representation allows the three-dimensional visualization of how the FHA changes position in space in relation to the TMJs during movements [Figure 2].

Briefly put, JAWS-3D uses three one-dimensional charge-coupled cameras, disposed in a fixed geometry, to track the spatial position of two triplets of light-emitting diodes (LEDs).[21] These diodes are disposed at the vertices of two triangular target frames (TTFs), rigidly connected to the upper and lower dental arches by means of custom made metal clutches [Figure 3]. The maxillary TTF determines the absolute movement of the head and mandibular TTF that of the mandible. By computing the motion of the mandible in relation to the head, head movements are eliminated and joint movements are obtained. The TMJ is imaged together with reference system by means of magnetic resonance.

These two triangular target frames, carrying three light-emitting diodes (LEDs) each defined a head related XYZ coordinate system and a mandible-related UVW coordinate system [Figure 2]. Both target frames positioned as close as possible to the TMJ, had the long axis parallel to the camper plane, while the Z axis was parallel to the sagittal plane and the W axis perpendicular to it.

For calculation of the position of the finite helical axis in relation to an intracondylar point, the lateral condylar pole was palpated and marked on the skin. After a LED was positioned over the marked point, the coordinates of this point were recorded by JAWS -3D in the mandibular UVW coordinate system

The W-coordinate was changed by 15 mm in the medial direction to obtain a point within the condyle. A 15mm correction was judged sufficient to obtain a point within the condyle.[22]

Once the target frames were mounted and the intracondylar point recorded, the subject, who sat in a conventional dental chair with the head unsupported, performed a series of three consecutive maximum open/close cycles with a 1 Hz frequency i.e., one open-close cycle in one sec [Figure 4]. The movements had to start and end in maximum intercuspation. The velocity of the open-close cycles was paced by a vertical LED array placed in front of the subject. Recordings started after the subject had learned to open and close at the paced velocity. The target frames were then removed and remounted on the other side. After the coordinates of the intracondylar point of this side were determined, a new series of three open-close cycles was registered. All movements were recorded in one session.

The calculation of the total rotation around the FHA, of the extreme positions and orientations of the FHA in relation to a preselected condylar point and of the global fluctuation of the FHA spatial orientation describes quantitatively the FHA pathway

DATA ANALYSIS

The jaw motion data were recorded on floppy discs and analyzed off-line by means of a PC-based computer and interactive software.

The mandibular movements were computed by modelling the mandible as a rigid body. This was done by determining the time dependent rotation matrix, $R(t_i)$, and the translation vector, $v(t_i)$, for the displacement of any mandibular point from one sampled position, $x(t_i)$, to the following one, $x(t_{i+1})$, so that

$$x(t_{i+1}) = R(t_i)\, x(t_i) + v(t_i)$$

from each rotation matrix and translational vector, defined at 14-ms intervals (71Hz). The whole motion of the mandible could be described as a combination of a translation, $\Delta T(t_i)$, along a finite helical axis and a rotation, $\Delta\Phi(t_i)$, around it. The finite helical axis with origin $s(t_i)$ and orientation $n(t_i)$ was calculated from the components of $R(t_i)$ and $v(t_i)$[20] the rotation, $\Delta\Phi(t_i)$

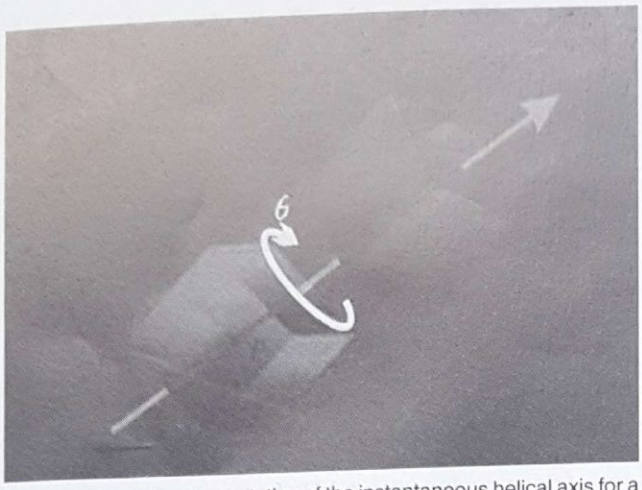

Figure 1: Graphic representation of the instantaneous helical axis for a cube moving in space (courtesy—A Textbook on Science and Practice of Occlusion—Charles McNeill)

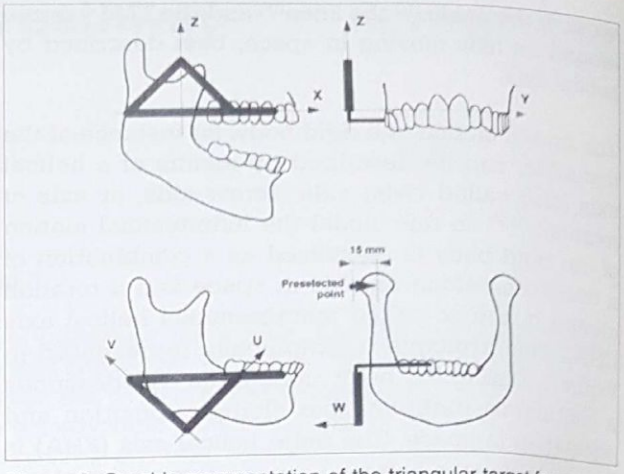

Figure 2: Graphic representation of the triangular target frames with the XYZ and UVW coordinates

Figure 3: Subject with two triangular target frames. Each triangle carries three LEDs and is attached to the upper and lower dental arch by means of a thin metal rod (courtesy—A Textbook on Science and Practice of Occlusion—Charles McNeill)

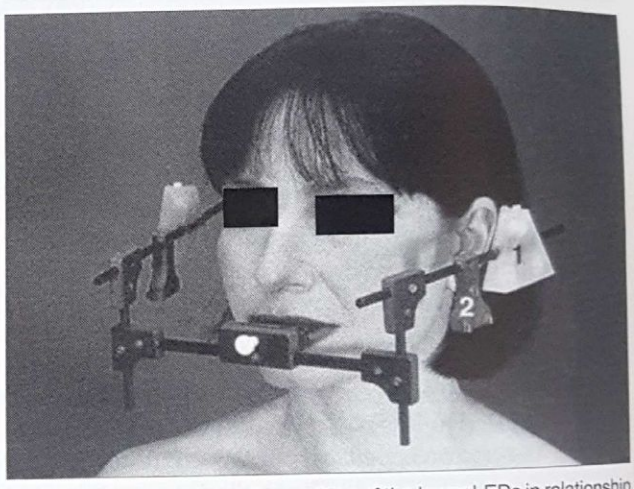

Figure 4: Setup to record the position of the lower LEDs in relationship to the reference system. The mandibular triangular target frame (1) is attached to the mandible, while another (2) is fixed to the framework. A condylar point is selected by means of an extra-oral pointer with the LED positioned over the palpated lateral condylar pole. (courtesy—A Textbook on Science and Practice of Occlusion—Charles McNeill)

around the finite helical axis and the translation, $\Delta T(t_i)$, along it were calculated for each sample time except when very small rotation angles occurred between consecutive motion steps. A threshold rotation value was set empirically to 1^0, below which the finite helical axis was not defined, since the distance of the finite helical axis from the condyle increases dramatically for very small rotation angles. For these motion steps, the movement was considered to consist only of translation.

For each sample time in which the finite helical axis was defined, the following parameters were calculated:

the vector $d_{CP}(t_i)$, pointing from the preselected condylar point perpendicularly to the finite helical axis [Figure 5] as well as the angles $\Phi x(t_i)$, $\Phi y(t_i)$ and $\Phi z(t_i)$ between the finite helical axis orientation, $n(t_i)$, and the references axes XYZ.

the instantaneous values $\Delta\Phi(t_i)$, $\Delta T(t_i)$, $d_{CP}(t_i)$, $\Phi x(t_i)$, $\Phi y(t_i)$ and $\Phi z(t_i)$ were used to calculate the following parameters [Figure 5]: the total rotation around the finite helical axis in degrees (Φ_{max}); the maximum translation along the finite helical axis in mm (T_{max}); the maximum distance between the finite helical axis and the selected condylar point in mm ($d_{CP\,max}$), i.e., the length of the longest vector, $d_{CP}(t_i)$; the maxima and minima of the components $Xd(t_i)$ and $Zd(t_i)$ of $d_{CP}(t_i)$ (x_{dmax}, x_{dmin}, z_{dmax} and z_{dmin}) in mm; the mean angles Φx, Φy and Φz as well as the mean global fluctuation of the the finite helical axis spatial orientation (Φe) in degrees.

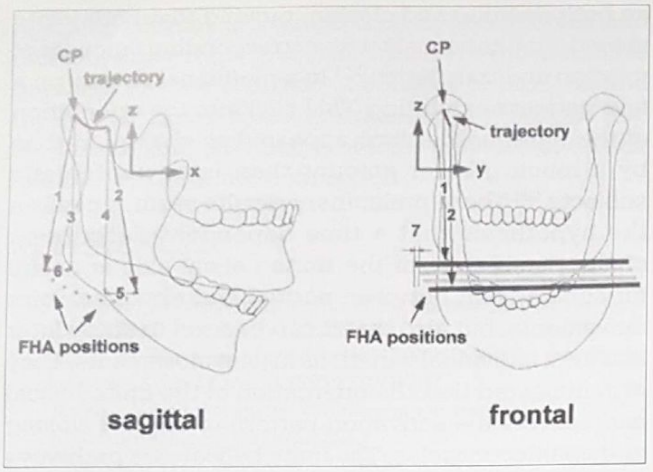

Figure 5: Description of FHA parameters: (1) vector dcp(ti) at maximum intercuspation: its length is the distance dcp(ti) between the FHA and the preselected condylar point CP. (2) vector dcp(ti) at maximum opening. (3) z dmax is the most cranial Z- component of dcp(ti). (4) z dmin is the most caudal Z- component of dcp(ti). (5) x dmax is the most frontal X - component of dcp(ti).(6) x dmin is the most dorsal component of dcp(ti). (7) Translation ΔT(ti) along the FHA for each sample time: the maximum of the integral of ΔT(ti) over time [T (ti)] is the maximum translation along the FHA (T max). The size of ΔT(ti) is exaggerated.

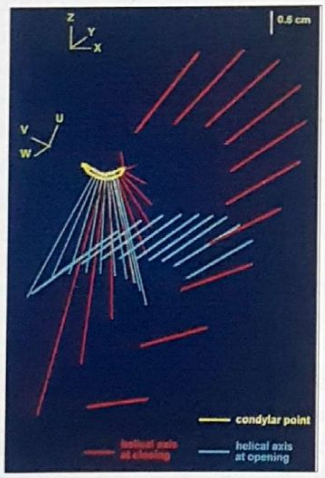

Figure 6b: Perspective views of the FHA pathway during the opening and closing phase of a chewing cycle. The FHA segments on opening are more parallel to each other than on closing. The FHA segments on closing vary more in their orientation in space from the beginning to the end of the movement than the FHA segments on opening

The computer also provided the three dimensional trajectory of the movement of the condylar point as well as a perspective representation of the movement of a segment of the finite helical axis.

The total rotation around the finite helical axis (Φ_{max}) corresponded to the maximum of $\Phi(t_i)$ that was computed by integrating $\Delta\Phi(t_i)$ over time. The integration sign was positive in the opening phase and negative in the closing phase. Opening and closing

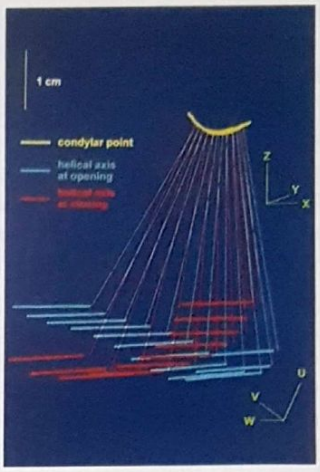

Figure 6a: Perspective view of the FHA pathway of a subject during an open-close cycle. UVW: mandibular coordinate system. XYZ: head related coordinate system. Both the FHA and condylar paths run from left to right; i.e., the movement starts on the left. The distances between the condylar point and the FHA segment are represented by the vector lines. Note that the FHA segments are always parallel to each other and describe a smooth pathway.

were distinguished by means of the Y- component of the finite helical axis (positive while opening and negative while closing). Similarly the maximum translation along the finite helical axis (T_{max}) corresponded to the maximum of $T(t_i)$ that was computed by integrating $\Delta T(t_i)$ over time. This value is a measure of the displacement of the mandible, mainly in the medio-lateral direction [Figure 5]. The integration sign to calculate $T(t_i)$ was positive in the opening phase and negative in the closing phase. Also for this parameter, opening and closing were distinguished by means of the Y-component of the finite helical axis. Figure 5 shows, in a frontal view, the displacement $\Delta T(t_i)$ of a finite helical axis segment in different positions due to a lateral deviation of the mandible during the opening/ closing movements.

The vector $d_{CP}(t_i)$ was used to quantify the spatial position of the finite helical axis with respect to the selected condylar point in the XYZ coordinate system at each motion step [Figure 5]. The length of the vector $d_{CP}(t_i)$ was the distance $d_{CP}(t_i)$, and its maximum length during the full movement cycle was the distance $d_{CP\,max}$. x_{dmax} and x_{dmin} represented the most vertical and the most dorsal components of $d_{CP}(t_i)$ during an entire movement cycle, whereas z_{dmax} and z_{dmin} represented its most cranial and most caudal components. These four parameters described the maximum displacements of the finite helical axis in the XZ-plane relative to the condyle within which the finite helical axis moved.

The mean global fluctuation of the spatial orientation of the finite helical axis (Φe) was calculated by averaging

$$\Phi e(t_i) = \sqrt{[\Phi x(t_i) - \Phi x]^2 + [\Phi y(t_i) - \Phi y]^2 + [\Phi z(t_i) - \Phi z]^2}$$

over all sample times t_i in which the finite helical axis was defined. Φe indicated the degree of parallelism of the finite helical axis i.e., if the finite helical axis remained parallel to itself during the mandibular movements. Φe is zero if the finite helical axis remains perfectly parallel to itself during the entire movement and increases the more it deviates from its mean orientation.

The global fluctuation Φe of the finite helical axis is a useful parameter for between individual comparision of the orientation of the pathway of the finite helical axis, since this value reflects the degree of parallelism between consecutive axes.

The global fluctuation of the FHA spatial orientation for open-close movements is small (4 +/- 2 mm), indicating a small irregularity of the FHA orientation during the opening and closing movements in all subjects. The FHA was located dorsoventrally to the working condyle and near or sometimes above the balancing condyle at the beginning of closing. At the end of the movement the FHA was next to the working condyle and dorsocaudally from the balancing condyle. This significant change in the orientation of the FHA during closing is most likely due to the timing difference in the movement of both the condyles during closing [Figure 6].

During functional movements the FHA's are never located within the condyles and they are often located outside of the mandible. In a sample of normal subjects the FHA's moved during empty open-close movements within a rectangle of 32 x 56 mm positioned inferiorly and most ventrally to the preselected condylar point. This finding confirms the results of previous two-dimensional models showing that the instantaneous centre of rotation lies outside the condyle.[23-26] These models also explain why the hinge axis cannot describe a pure translatory movement during functional movements. The distance of the FHA's from the condyle varies between subjects, probably depending on joint and skeletal morphology as well as muscle recruitment. Obviously, the form of the path described by condylar points during movements is directly influenced by its distance from the FHA. This explains why the geometric errors in condylar point tracings may be more pronounced in one individual than in another.

The mandibular finite helical axes always described a smooth pathway on both opening and closing, showing neither sudden nor irregular changes in position and orientation. These results indicate a high degree of parallelism between consecutive finite helical axes on both opening and closing, proving that both joints moved simultaneously with corresponding amounts of rotation and translation.[27] In a preliminary study on a few patients exhibiting TMJ clicking, the orientation of the finite helical axis appeared to change in time by a much greater amount than in asymptomatic subjects.[28] These preliminary results seem to confirm the hypothesis that a time dependent description of the parameters of the finite helical axis is useful for comparision between normal and abnormal joint movements, but also that it can be used to study inter and intra individual variations in joint movements. They also indicated that the orientation of the finite helical axis reflects the activation pattern of the jaw closing and opening muscles. The finite helical axis pathways in subjects with clicking joints appeared to fluctuate more and move in a larger space than in asymptomatic subjects.

Finite helical axis pathways were recorded for asymptomatic subjects and subjects with TMJ clicking.[29]

Following parameters were calculated: the rotation of the FHA, its spatial orientation, the translation along it as well as the FHA position and distance relatively to an intracondylar point. In asymptomatic subjects the group mean FHA rotation was 24.3^0 + or -4.2^0. The group mean of the maximum total translation along the FHA was 0.9+ or -0.7 mm; The group mean distance between the FHA and the intracondylar point was 48.9+ or -9.9 mm. The FHA pathways of asymptomatic subjects were smooth and varied interindividually whereas subjects with clicking showed strong deviations of the FHA orientation

In general the opening and closing pathways did not coincide in the same subject. This noncoincidence of the finite helical axis pathways is most likely due to the asymmetrical combination of rotations and translations during opening and closing, since different muscles are used to open and close the mandible

CONCLUSION

The finite helical axis pathways contain information on both the amounts of rotation and translation of the mandible,[30] thus yielding a more comprehensive description of jaw movements than do the trajectories of a single mandibular point.

The helical axis does not contain mere kinematic information. Knowledge of the helical axis is a first step toward the dynamic analysis of joint loading. The forces acting on a joint mostly generate rotatory movements occurring around the helical axis. The

resulting torques are the product of linear forces and moment arms of the muscles, which are the distances between the line of action of muscles or tendons and the helical axis[31] moment arms give an insight into the mechanical advantage of joint muscles and their relative contribution to an action.

REFERENCES

1. Rocabado M. Arthrokinematics of the temporomandibular joint. Dent Clin North Am 1983;27:573-94.
2. Smith RJ. Functions of condylar translation in human mandibular movement. Am J Orthod 1985;88:191-202.
3. Rayne J. Functional anatomy of the temporomandibular joint. Br J Oral Maxillofac Surg 1987;25:92-9.
4. Freesmeyer WB, Stehle CM. Biomechanics of temporomandibular joint movements. Dtsh Zahnarztl Z 1988;43:199-208.
5. Pertes RA, Attanasio R, Cinotti WR, Balbo M. The temporomandibular joint in function and dysfunction. Clin Prev Dent 1988;10:23-9.
6. McKay GS, Yemm R, Cadden SW. The structure and function of the temporomandibular joint. Br Dent J 1992;173:127-32.
7. Gallo LM, Salaorni C, Airoldi RL, Palla S. Classification of anterior displacement vs. condylar rotation patterns in healthy TMJs (abstract). J Dent Res 1993;(spec issue)72:372
8. Pullinger AG, Liu SP, Low G, Tay D. Differences between sexes in maximum jaw opening when corrected to body size. J Oral Rehabil 1987;14:291-9.
9. Westling L, Helkimo E. Maximum jaw opening capacity in adolescents in relation to general joint mobility. J Oral Rehabil 1992;19:485-94.
10. Posselt U. Physiology of occlusion and rehabilitation ed. 3. London: Blackwell; 1966. p. 40.
11. Merlini L, Palla S. The relationship between condylar rotation and anterior translation in healthy and clicking temporomandibular joints. Schweiz Monatsschr Zahnmed 1988;98:1191-9.
12. Salaorni C, Palla S. Conylar rotation and anterior translation in healthy human temporomandibular joints. Schweiz Monatsschr Zahnmed 1994;104:415-22.
13. Gallo LM, Airoldi GB, Airoldi RL, Palla S. Description of mandibular finite helical axis pathways in asymptomatic subjects. J Dent Res 1997;76:704-13.
14. Wilson DL, Zhu Q, Duerk JL, Mansour JM, Kilgore K, Crago PE. Estimation of tendon moment arms from three-dimensional magnetic resonance images. Ann Biomed Eng 1999;27:247-56.
15. Chen J, Siegler S, Schneck CD. The three dimensional kinematics and flexibility characteristics of the human ankle and subtalar joint, part 2: flexibility characteristics. J Biomech Eng 1988;110:374-85.
16. Hart RA, Mote CD Jr, Skinner HB. A finite helical axis as a landmark for kinematic reference of the knee. J Biomech Eng 1991;113:215-22.
17. de Lange A, Huiskes R, Kauer JM. Measurement errors in roentgenstereophotogrammetric joint motion analysis. J Biomech 1990;23:259-69.
18. Ramakrishnan HK, Kadaba MP. On the estimation of joint kinematics during gait. J Biomech 1991;24:969-77.
19. Siegler S, Chen J, Schneck CD. The three dimensional kinematics and flexibility characteristics of the human ankle and subtalar joints-part 1. J Biomech Eng 1988;110:364-73.
20. Spoor CW, Veldpaus FE. Rigid body motion calculated from spatial coordinates of markers. J Biomech 1980;13:391-93.
21. McNeill C. Science and practice of occlusion ed 1. Quintessence; 1997. p. 374-6.
22 Krenkel C, Grunert I. The mandibular condyles in the Rundstrom IV radiograph – their relationship to hinge axis and the significance of the condylar axis in transcranial TMJ radiography. Z Stomatol 1988;85:135-53.
23. Baragar FA, Osborn JW. A model relating patterns of human jaw movement to biomechanical constraints. J Biomech 1984;17:757-67.
24. Grant PG. Biomechanical significance of the instantaneous centre of rotation: the human temporomandibular joint. J Biomech 1973;6:109-13.
25. McMillan AS, McMillan DR, Darvell BW. Centres of rotation during jaw movements. Acta Odontol Scand 1989;47:323-8.
26. Nattestad A, Vedtofte P. Mandibular autorotation in orthognathic surgery: a new method of locating the centre of mandibular rotation and determining its consequence in orthognathic surgery. J Craniomaxillofac Surg 1992;20:163-70.
27. Airoldi GB. Three dimensional description of mandibular finite helical axis pathways in asymptomatic subjects (medical dissertation). Zurich,1994.
28. Gallo LM, Ernst B, Palla S. Relevance of mandibular finite helical axis analysis in clicking joints. J Dent Res 1997;76(spec issue):446.
29. Gallo LM, Airoldi GB, Palla S. Finite helical axis description of functional movements of the mandible- Computer methods in biomechanics and biomedical engineering. Gordon and bridge: New York and London; 1996. p. 441-51.
30. Gallo LM, Fushima K, Palla S. Mandibular helical axis pathways during mastication. J Dent Res 2000;79:1566-72.
31. Boyd SK, Ronsky JL. Instantaneous moment arm determination and flexibility characteristics of the human ankle and subtalar joint- part II: flexibility characteristics. J Biomech Eng 1988;110:374-85.

Source of Support: Nil, **Conflict of Interest:** None declared.